



The rise of stratification – Climate-induced changes in the thermal structure of a shallow polymictic lake until 2100

Sebestyén Dániel Török^{1,2}, Márk Honti^{2,3}, Péter Torma^{1,2,4}

¹Department of Hydraulic and Water Resources Engineering, Budapest University of Technology and Economics, Budapest, Hungary

²National Laboratory for Water Science and Water Security, Budapest University of Technology and Economics, Faculty of Civil Engineering, Department of Hydraulic and Water Resources Engineering, Budapest, Hungary

³HUN-REN-BME Water Research Group, Budapest, Hungary

⁴HUN-REN-SZTE Research Group for Photoacoustic Monitoring of Environmental Processes, Szeged, Hungary

10 *Correspondence to:* Sebestyén Török (toroks@edu.bme.hu)

Abstract. Climate change exerts a significant influence on lake ecosystems by altering stratification and thermal dynamics. These changes are commonly quantified using climate model projections to assess future conditions. However, climate model simulations generally have a daily temporal resolution, which is inadequate for resolving the fast, sub-daily processes governing shallow lakes. Consequently, long-term impacts of climate change on shallow lakes remain underrepresented in literature. This study presents a modeling workflow for simulating and quantifying future climatic conditions in shallow environments, where sub-daily resolution is necessary. The proposed workflow comprises a weather generator for the temporal downscaling meteorological forcing, as well as a physics-based one-dimensional model for simulating lake thermal dynamics. The workflow is applied to Lake Balaton, a large polymictic lake, to assess the effects of the projected climatic changes on the lake through the end of the century. Changes are analyzed as a function of time and water depth, under the RCP4.5 and RCP8.5 climate scenarios, using an ensemble of 14 climate model simulations. Our findings indicate that stratification is likely to intensify throughout the century, in a complex interplay with water depth, in which mutually enhancing effects are accompanied by progressive dampening. The number and duration of stratified events show a slight increase, which does not reflect the magnitude of the projected intensification in stratification, suggesting that wind forcing remains a dominant factor in regulating stratification dynamics. Lastly, the evaluation of lake heatwaves using a temporally varying baseline indicates no significant changes in their characteristics.

1 Introduction

Lakes are often referred to as sentinels of climate change, as they exhibit rapid and diverse variations in response to climatic shifts (Adrian et al, 2009). Among these changes, the lakes' thermal structure is particularly sensitive, with frequently observed shifts in stratification patterns, increased surface temperatures, and altered mixing regimes (Woolway et al., 2020; 2021b). Thermal stratification plays a crucial role in lake ecosystems as the mixing regime controls the vertical transport of oxygen and nutrients. Prolonged stratified periods usually limit the oxygen supply to the lower water layers, which leads to a regularly anoxic hypolimnion in many deep lakes but in extreme cases can cause oxygen depletion in shallow lakes too (Shi et al., 2022;



Jane et al., 2021). In shallow lakes, these conditions can increase the risk of algal blooms and may lead to water quality problems (Istvánovics et al., 2022; Salmaso, 2005). Climate change generally increases thermal stability (Fukushima et al., 2022) even in polymictic lakes, promoting stronger and more persistent stratified periods, consequently increasing the likelihood of adverse ecological impacts. However, the magnitude of these changes remains uncertain in the long term, as it depends heavily on the trajectory of future climatic conditions.

To represent this climatic uncertainty, the Intergovernmental Panel on Climate Change (IPCC) introduced four Representative Concentration Pathway (RCP) scenarios, each reflecting different projections of greenhouse gas emissions, to estimate the range of potential changes by the end of the century (IPCC, 2014). Among these, due to the actual development of GHG emissions, RCP4.5 and RCP8.5 are commonly employed scenarios; RCP4.5 – formerly considered as a realistic pathway – represents an intermediate stabilization with moderate mitigation efforts leading to a projected global mean surface temperature increase of 1.1-2.6 °C (this turned out to be overly optimistic in the last 10 years), whereas RCP8.5 corresponds to a high-emission – formerly pessimistic, now realistic - trajectory associated with an expected rise of 2.6-4.8 °C, often considered extreme. The scenarios do not represent likelihoods but rather serve as guidance for the policy maker to inform their decision (Schwalm et al., 2020). These scenarios are commonly employed to quantify potential changes in lake environments (Woolway et al., 2021b; Shatwell et al., 2019). However, shallow lake systems are relatively underrepresented in studies (Sahoo et al., 2016).

The shallowness increases a lake's susceptibility to external changes, because the dampening effect of the water mass is limited. Therefore, shallow lakes generally respond faster to meteorological forcing – hence are they polymictic – and they are more sensitively to climate change and anthropogenic effects. In deep lakes, thermal stratification typically persists for several weeks to months, sometimes years, while in shallow lakes it generally ranges from hours to days. This occurs because of the lower stability of the water column, resulting from temperature-induced density differences, allowing current- and wind-induced mixing to disrupt stratification more consistently (Martinsen et al., 2019; Torma & Krámer, 2017; Kimura et al., 2016). Consequently, relatively elevated water levels can substantially enhance thermal stability in shallow environments (Kraemer et al., 2015). The expected increase in extreme meteorological and hydrological conditions during climate change increases water level variability even in regulated lakes (Woolway et al., 2020), leading stakeholders to pursue higher levels to provide a buffer against potential declines in lakes' water balance (La Fuente et al., 2024). However, such management may enhance the likelihood of prolonged stratified periods and the risk of oxygen depletion even in very shallow, polymictic environments (Istvánovics et al., 2022).

The detection of the volatile stratification events is difficult in shallow polymictic lakes; therefore, a sub-daily resolution is necessary to capture stratification dynamics accurately. In contrast, climate models provide reliable estimates on a daily resolution at most, necessitating the downscaling of these data to model intra-daily processes (Smith et al., 2025). Studies projecting changes in shallow lakes provide only limited insight into stratification, either because it is not their primary focus or because the modeling resolution is insufficient to capture these processes accurately. Cui et al. (2025) examined the future impacts of climate change on Lake Taihu's thermal and ecological conditions by the end of the century, with stratification



variations assessed indirectly. Their simulations indicate a weakening of winter stratification, but the summer vertical thermal structure was not analyzed comprehensively. Hetherington et al. (2015) investigated the impacts of climate change on the thermal structure of Oneida Lake, a shallow polymictic lake in New York, USA, projecting more extended consecutive stratified periods by the end of the century with prolonged summer stratifications. However, the simulations driven by projected climate data were conducted at a daily time step, and stratification was inferred indirectly from modelled water temperatures. Schwefel et al. (2025) examined projected changes of 12 lakes in Germany until 2099, comprising one polymictic and eleven stratified systems. Their results indicate an overall intensification and extension of summer stratification by 38 days, characterized by earlier onset, delayed autumnal mixing, and a shortened duration of winter stratification. Nevertheless, sub-daily stratification dynamics were not considered and therefore the prognoses for the polymictic system may be biased. To summarize, the projected long-term impacts of climate change on the stratification of shallow, polymictic lakes remain largely unexplored, with sub-daily variations being scarcely investigated.

To bridge this gap, the aim of our study is to present a methodology for simulating sub-daily thermal dynamics in polymictic environments, given that future meteorological projections are generally limited to daily or coarser resolutions. To this end, we developed a modeling workflow that is capable of downscaling meteorological data to sub-daily resolution and subsequently simulates the thermal regime of water. In addition, the study provides a comprehensive assessment and quantifies the projected long-term impacts of climate change on the temperature dynamics of a large yet shallow lake, namely Lake Balaton (Central Europe), until the end of the century. We analyze changes in stratification in terms of intensity, duration, and its dependence on water depth under two climate scenarios, based on an ensemble of 14 climate model simulations. Furthermore, the projected changes in the occurrence of lake heatwaves are quantified. Analyses are conducted at sub-daily resolution using the proposed modeling framework, capturing diurnal variability in the processes studied. The results form a basis for further investigations on the stratification-water quality coupling in shallow lakes, as the progression of climate change affects an increasing number of lakes.

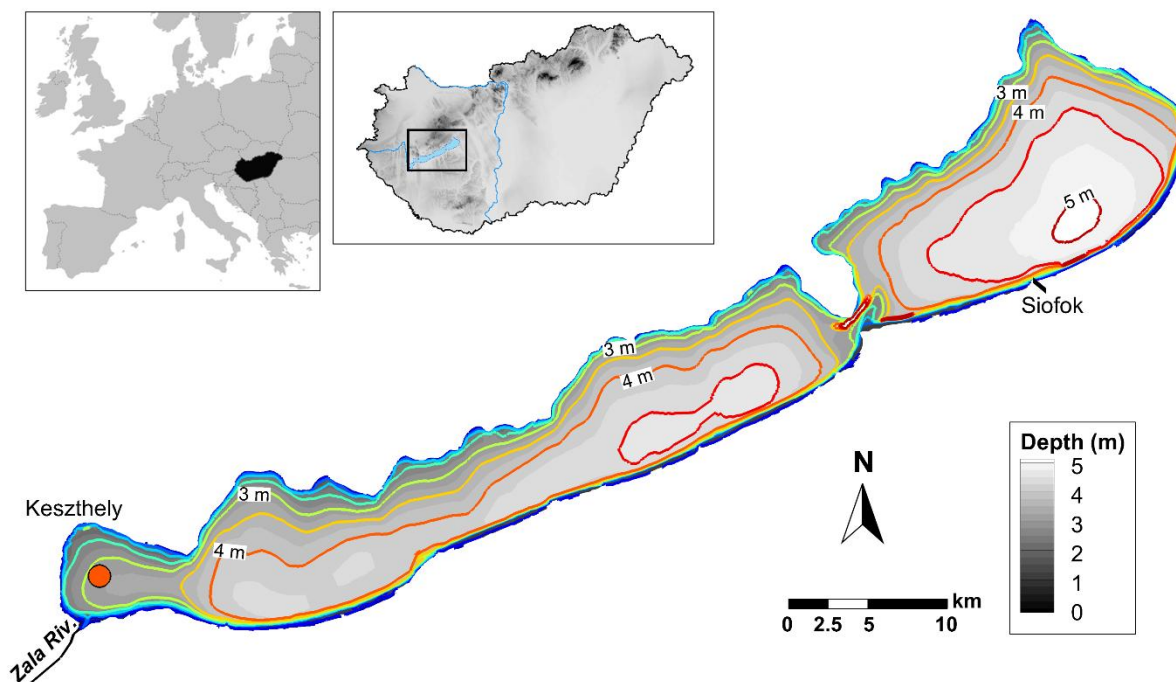
2 Materials and methods

2.1 Study site and supporting data

Lake Balaton is the largest lake in Central Europe, with a surface area of 596 km² (Fig. 1). It is classified as a shallow polymictic lake due to its mean depth of 3.5 m. The lake has an elongated shape and, in terms of its hydrodynamic behavior and water-quality patterns, is usually delineated into four distinct basins (Istvánovics & Honti, 2018). The lake's main inflow, River Zala, enters the westernmost basin, collecting the runoff from half of its total catchment area (5180 km²), while the lake's outflow, which is regulated, is in the easternmost basin. Before entering Lake Balaton, the river traverses a large, restored wetland system that markedly reduces its sediment loads and flow velocities, with the decreased velocities causing the throughflow to exert only a very local and generally negligible influence on the lake's stratification regime. Therefore, the thermal



stratification of the lake is primarily shaped by local meteorological forces, which, due to the lake's shallowness, typically lead to weak diurnal stratifications (Török & Torma, 2025).



100

Figure 1: Location and bathymetry of Lake Balaton, with the measurement site marked by an orange dot.

Meteorological input data for the modeling were supplied from the ECMWF ERA5 reanalysis and the FORESEE climate databases (Kern et al., 2024; Dobor et al., 2015). The former was used to train the weather generator to downscale daily meteorological data into 6-hour resolution (details are provided in the following section), whereas the latter was applied to simulate both present conditions (2000–2020) and future scenarios for 2040–2060 and 2080–2100, representing the projected near- and far-future changes. The FORESEE climate database is an open-access meteorological dataset providing observed and projected daily data for the Carpathian Basin, in which the entire the catchment is located. Projections are based on 14 EURO-CORDEX regional climate model chains under the RCP 4.5 and RCP 8.5 scenarios (Kern et al., 2024). The database includes daily precipitation (P_r) and minimum and maximum air temperatures, from which daily mean air temperature (T_a) was calculated. These data were then used to derive the variables required for the stratification modeling – the wind speed (U), incoming shortwave radiation (SW_{in}), air temperature (T_a), and relative humidity (RH) – through the downscaling process. To train the models, ECMWF data were used – where T_a and U were bias-corrected based on field measurements – instead of the FORESEE dataset as they were available at an hourly resolution and had already been proven reliable for Lake Balaton (Török & Torma, 2024). A preliminary assessment of the ECMWF and FORESEE datasets demonstrated a high degree of consistency across the variables. Regarding precipitation, FORESEE data exhibited an underestimation of approximately 20% relative to

115

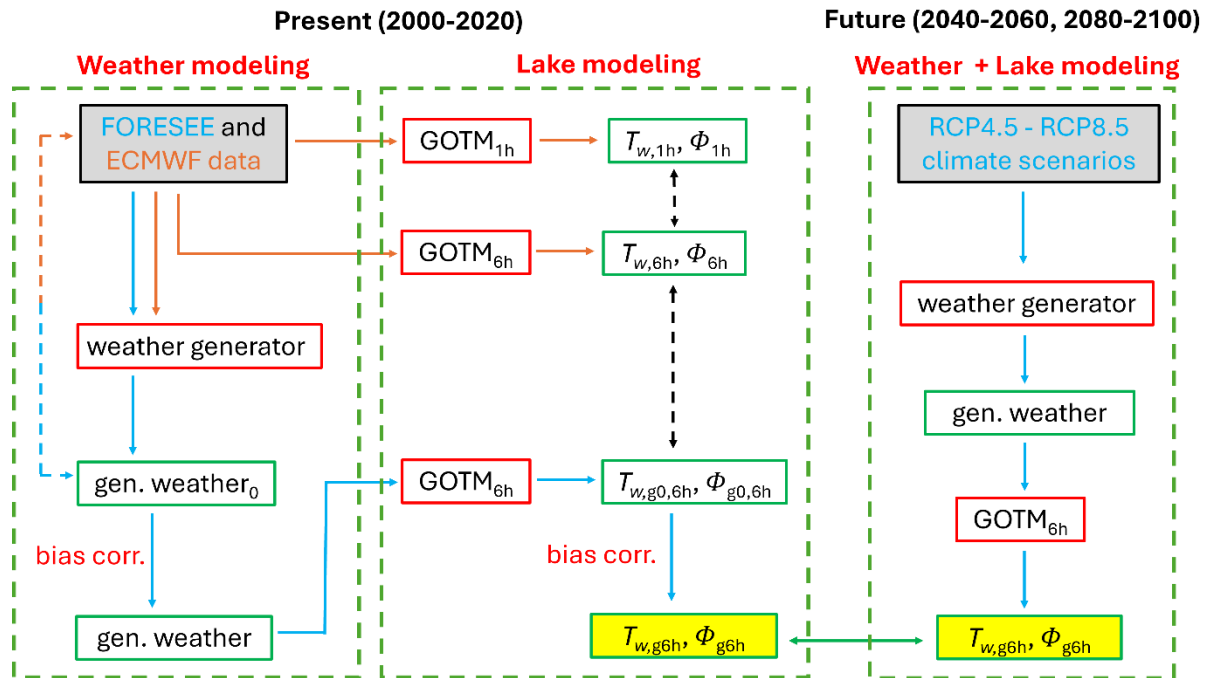


the ERA5 dataset; however, as the projected changes were quantified relative to the base period and future changes are assumed to scale linearly from the baseline, this bias did not influence the results.

2.2 Modeling workflow

120 An important prerequisite of our analysis was to produce suitable sub-daily meteorological data for the simulation of future temperature profiles in Lake Balaton. To do this, gaps in the resolution and extent of the above-mentioned meteorological databases had to be bridged. While ECMWF is rich in variables and has an hourly resolution, it does not have forecasts for the far future. On the other hand, FORESEE spans from the distant past to the end of this century, yet at a mere daily resolution and only for the most basic variables. We resolved this – rather usual – forecasting issue by applying stochastic downscaling for future data with a weather generator that was trained to reproduce the past high-resolution ECMWF data from the past
125 daily FORESEE variables.

The model system consists of three submodules (Fig. 2). The role of the first submodule was to generate meteorological data by stochastic downscaling, as well as to assess their reliability, required for modeling the present stratification conditions. For this purpose, daily air temperatures and precipitation were used as inputs for a weather generator to downscale and generate the necessary variables at a 6-hour resolution. In the training process, ERA5 data were employed as inputs, while daily
130 FORESEE data were used to generate the present meteorological conditions. The resulting downscaled outputs were systematically compared to the corresponding 6-hourly values derived from hourly ECMWF data for all variables. To address the discrepancies between datasets, a bias correction was applied to the downscaled datasets by aligning their cumulative distribution functions with the 6-hourly ECMWF data using second-degree polynomials. Thereafter, both the ECMWF and downscaled FORESEE datasets were employed as inputs to the second submodule, which was designed to simulate
135 stratification dynamics. When derived from ECMWF data, they served to assess the impacts of reduced temporal resolution. Conversely, those derived from FORESEE data – bias-corrected using the transfer functions obtained from the ECMWF-based calibration – provided the reference baseline for evaluating projected future changes.



140 **Figure 2: Schematic representation of the modeling process. Grey-shaded boxes with black borders represent input data, while red-bordered boxes indicate modeling steps and green-bordered boxes denote intermediate results. Blue and brown colors correspond to the FORESEE and ECMWF datasets, respectively, with arrows of matching color showing their use within the modeling framework. Yellow-shaded boxes with green borders represent the results compared at the end of the process. Dashed lines indicate comparison steps, while the abbreviation “bias corr.” refers to bias correction, an intermediate step within the modeling workflow.**

In the second submodule, the depth-averaged mean water temperature (T_w) and the potential energy anomaly index (ϕ) – a
 145 quantitative measure of stratification intensity (Wiles et al., 2006) – are calculated from water temperature profiles computed along the water column using the one-dimensional General Ocean Turbulence Model (GOTM). Changes between present and future conditions are evaluated using these two indicators; consequently, T_w and ϕ values calculated from the hourly ECMWF dataset, the six-hourly ECMWF dataset, and the six-hourly downscaled FORESEE dataset were compared to assess if the reduced temporal resolution was sufficient to derive representative values (Table 1). For this, a bias correction was applied to
 150 both variables, consistent with the process employed in the first submodule for the meteorological variables. The bias-corrected T_w and ϕ results – for the generated present – are subsequently used to characterize the present conditions of Lake Balaton. The model system's third submodule simulates projected future conditions for Lake Balaton, using the results of 14 regional climate models in FORESEE for the RCP4.5 and RCP8.5 climate scenarios (Kern et al., 2024). The first step of this process is downscaling, followed by bias-correcting the meteorological data required for modeling using the coefficients applied in the
 155 first submodule. In the next step, the depth-averaged mean water temperature and potential energy anomaly index are derived from GOTM simulations and bias-corrected using the coefficients from the second submodule for the examined periods (2040-2060 and 2080-2100), across the three predefined water depths and all model chains in both RCP scenarios. Finally, the simulated future conditions are systematically compared with the present conditions to assess the anticipated changes.



2.3 Weather generation

160 The weather generator was an extended version of the UKCP09 (or EARWIG) weather generator by Kilsby et al. (2007). The
standard version of EARWIG has daily resolution and contains two linked modules. The first module is a Neyman-Scott
Rectangular Pulse (NSRP, Rodriguez-Iturbe et al., 1987; Cowpertwait, 1991) model that generates downscaled precipitation
at hourly resolution, which can be later aggregated to daily level. The NSRP model represents precipitation as a stochastic
process in which rainfall events are generated by a Poisson process characterized by season-specific follow-up times. Each
165 event has a random cluster of rectangular rain cells, which in turn have their own relative starting points, duration and intensity.
Precipitation intensity can be calculated at any desired resolution from the superposition of rain cells, yet sub-hourly intensity
dynamics are usually poorly represented (Favre et al., 2004). The second module describes all other meteorological variables
by daily first-order autoregressive (AR) models. The set of meteorological variables is open; one only needs to ensure that
principal variables (daily mean air temperature and air temperature difference) are included. Besides the values of the preceding
170 day, the AR models consider the precipitation status of the current day (e.g. wet or dry day) and the current values of the
principal meteorological variables. The AR models are parameterized separately for each biweekly period and for different
weather transition conditions (based on the wetness state of the preceding and the current days).

While the standard version of this weather generator does not allow calculating sub-daily data for non-precipitation variables,
its general algorithm was still suitable for doing so due to the openness of the set of variables. As one can easily include e.g.
175 the daily maximum air temperature or cloud cover as a generic, non-principal variable. We have defined 6-hourly variables of
wind speed, incoming shortwave radiation, air temperature, and relative humidity in the same way.

The weather generator was trained on six-hourly ERA5 data for the period 2000–2020 as a reference. For the projection of
future trends until 2100, the daily climate change signals of principal variables between the historical (2000-2020) and future
(2040-2060; 2080-2100) periods were taken from FORESEE and applied as an adjustment of NSRP and AR parameters.

180 2.4 Lake modeling

The second submodule of the model system was responsible for the stratification simulations, which were carried out with the
one-dimensional General Ocean Turbulence Model, a physics-based water column model designed to describe the
hydrodynamic and thermodynamic processes in natural water bodies (Burchard et al. 1999). The model was driven by routine
meteorological variables, which include net solar radiation, wind speed, air pressure, air temperature, relative humidity, and
185 cloud cover. Among these, SW_{in} , U , T_a , and RH were provided by the first submodule, while net radiation was calculated
assuming a constant albedo of 0.08, and with cloud cover estimated from the ratio of incoming shortwave radiation to its value
for clear-sky conditions. For the modeling, the water depth was also needed. Therefore, to assess the depth-dependence of
stratification, three different but constant depths were considered: 2.98, 3.23, and 3.48 m, where the latter corresponds to the
latest maximum control level, the summer target. These depths are equivalent to lake gauge readings of 70, 95, and 120 cm,
190 respectively. In GOTM, vertical mixing was represented by a k - ϵ turbulence model, with Neumann (flux) boundary conditions



applied to the turbulent kinetic energy and dissipation rate equations. The corresponding upper and lower boundary fluxes were computed according to the logarithmic law of the wall, and a minimum eddy and heat diffusivity of $5 \cdot 10^{-6} \text{ m}^2 \text{ s}^{-1}$ was applied. Turbulent heat fluxes were calculated using the bulk formulas of Kondo (1975), while the longwave back radiation was determined following the approach of Clark et al. (1974). The sediment-water heat exchange was neglected in the model.

195 Observations from the 2019 measuring campaign indicated low summer sediment heat fluxes, with a mean of 5.91 W m^{-2} and a standard deviation of $\pm 3.92 \text{ W m}^{-2}$ (Török et al., 2023), suggesting that its omission is not expected to substantially influence the thermal dynamics of the water column. The light extinction coefficient was assumed to be temporally constant and set to 2.5 m^{-1} , based on measurements conducted by the Balaton Limnological Research Institute between 2022 and 2024 (Török & Torma, 2025). The potential anomaly index, which was used as a quantitative measure of the strength of stratification, was

200 calculated from the model-derived water temperature profiles as follows:

$$\phi = \frac{g}{h} \int_0^h [\bar{\rho} - \rho(z)] z dz, \quad (1)$$

where g (m s^{-2}) is the gravitational acceleration, h (m) is the water depth, $\bar{\rho}$ (kg m^{-3}) is the mean density of the water column, $\rho(z)$ (kg m^{-3}) is the water density at z depth, and z (m) is the vertical coordinate.

The model simulations covered the period from May to September; however, the analysis presented in this study is limited to

205 the summer months, as that is the ecologically most crucial period and it provides favorable conditions for developing enduring thermal stratification. It must be noted that GOTM does not allow the development of unstable stratification, the model immediately mixes the water column whenever such conditions arise, which can lead to a slight underestimation stratified duration. However, during summer, unstable stratification events are usually both short-lived and weak, so this bias is negligible. Additional details on the model setup, including the calibration and validation procedures and their results, are

210 provided in Török and Torma (2025, 2024).

2.5 Lake heatwaves

Lake heatwaves are considered extreme events characterized by the daily mean lake surface temperature exceeding the locally and seasonally dependent 90th percentile threshold for at least five consecutive days (Hobday et al., 2016). In the case of Lake Balaton, due to its shallowness, which leads to a weak vertical thermal gradient, the depth-averaged water temperature was

215 utilized in place of the surface temperature. The applied thresholds were defined relatively to baseline climatological means, calculated on a daily basis as follows: daily mean water temperatures were averaged within an 11-day window centered on each calendar day over the simulation period to ensure a sufficient sample size for percentile estimation. Then, the resulting values were smoothed with a 31-day moving average for a smooth climatological mean following Woolway et al. (2021a). Afterwards, events separated by at least three days were classified as distinct; otherwise, they were merged into a single event.

220 Lake heatwaves were analyzed separately for each modeling period, meaning that the changes in water temperature were assessed relative to the climatological mean calculated for their corresponding time, rather than being compared to the baseline climatology of present conditions.



3 Materials and methods

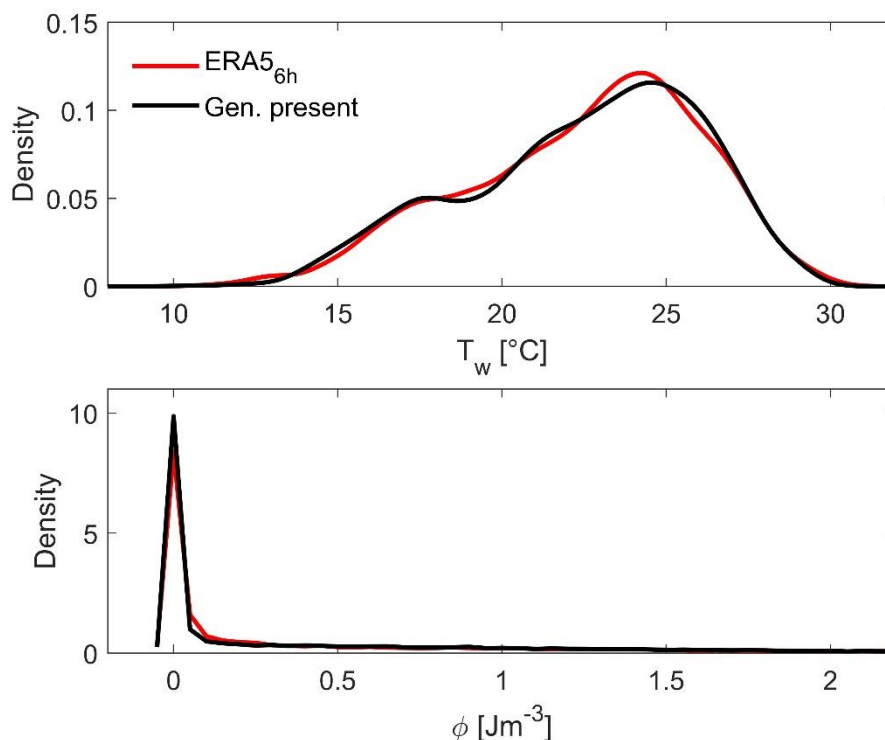
3.1 Validation of the temporal downscaling

225 We compared hourly and six-hourly water temperatures and potential energy anomaly indices for the present period, and found that using a lower time resolution for modeling the lake’s daily dynamics did not significantly affect primary statistical indicators – mean, median, and standard deviation (Table 1). However, a decrease in the amplitude could be discerned. For water temperature, differences of 0.1–0.2 °C were observed in the key indicators, while the maximum showed an overestimation of approximately 0.3 °C using the six-hour resolution. For potential energy, the statistical indicators remained
 230 largely consistent, except for the maximum, which exhibited an underestimation of 0.9 J m⁻³. These indicated that the extremes may have been over- or underestimated with the lower temporal resolution, but overall, the statistical consistency was preserved.

Table 1: Comparison of water temperature and potential energy anomaly statistics derived from the hourly ERA5, six-hourly ERA5, and FORESEE downscaled (generated) data for the baseline period of 2000-2020.

	Input data	min	max	mean	stdev	median
T_w [°C]	ERA5 _{1h}	10.9	30.0	22.4	3.5	22.9
	ERA5 _{6h}	10.9	30.3	22.5	3.6	23.1
	Gen. present	10.2	29.8	22.5	3.6	23.1
ϕ [Jm ⁻³]	ERA5 _{1h}	0	6.7	0.6	0.9	0.1
	ERA5 _{6h}	0	5.8	0.6	0.9	0.1
	Gen. present	0	6.3	0.6	0.9	0.1

235 Comparing the T_w and ϕ results obtained from the downscaled FORESEE meteorological variables with those derived from the ERA5 data showed good correspondence; the mean, median, and standard deviation were identical to those calculated from the six-hour dataset, whereas the minimum and maximum values exhibited slight deviations (Table 1). A high degree of consistency could be observed between the probability density functions of the two datasets (Fig. 3.), with only minor discrepancies, which are likely to be the result of the stochastic downscaling procedure. This indicates that, from a statistical
 240 perspective, the downscaling method performs adequately, as it could reproduce the distributions of the target variables along with the key indicators. However, some uncertainty remains, particularly in the representation of extreme values, which was handled by later phases of the model framework. Overall, the downscaling can be considered reliable and suitable for further subsequent analyses.



245 **Figure 3: Probability density functions (kernel density estimates) of water temperature and potential energy anomaly index derived from the six-hourly ERA5 data and FORESEE downscaled (generated) dataset for the period of 2000-2020.**

3.2 Climatic changes

The FORESEE database provides daily precipitation and the minimum and maximum air temperature, from which the daily mean air temperature was derived for the 14 climate models. Long-term series of air temperature between 1981 and 2100 showed an increasing trend (Fig. 4.), which, under the RCP4.5 scenario, persists until approximately mid-century, whereas under the RCP8.5, it continues until around the 2090s. In both cases, warming is followed by a slight decline thereafter. The trajectories of the two scenarios exhibit considerable similarity until the 2060s. However, after that, a substantial divergence develops. This suggests that only minor differences in water temperature and stratification can be expected between the scenarios in the near-future period, while more pronounced differences are likely to arise later in the century. Compared to the reference period, an increase of 0.98 °C and 1.00 °C in air temperature is projected for 2040-2060 under the RCP4.5 and RCP8.5 scenarios, respectively. By the end of the century, these changes are projected to be 0.87 °C and 3.01 °C, depending on the scenario considered.

There was no similar obvious change in summer precipitation sums. Projected changes in mean summer precipitation vary between -5 and +15 mm, which can be considered negligible compared to the present average of 192 mm/summer. This indicates that the expected significant changes in T_w and ϕ must be primarily driven by variations in air temperature.

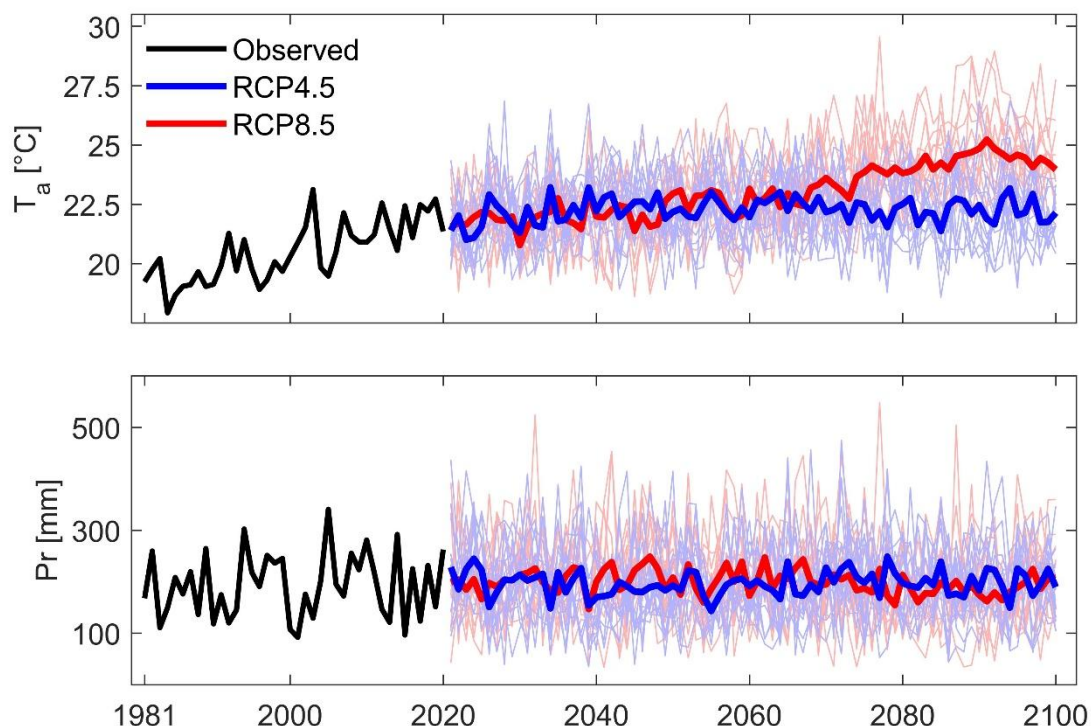
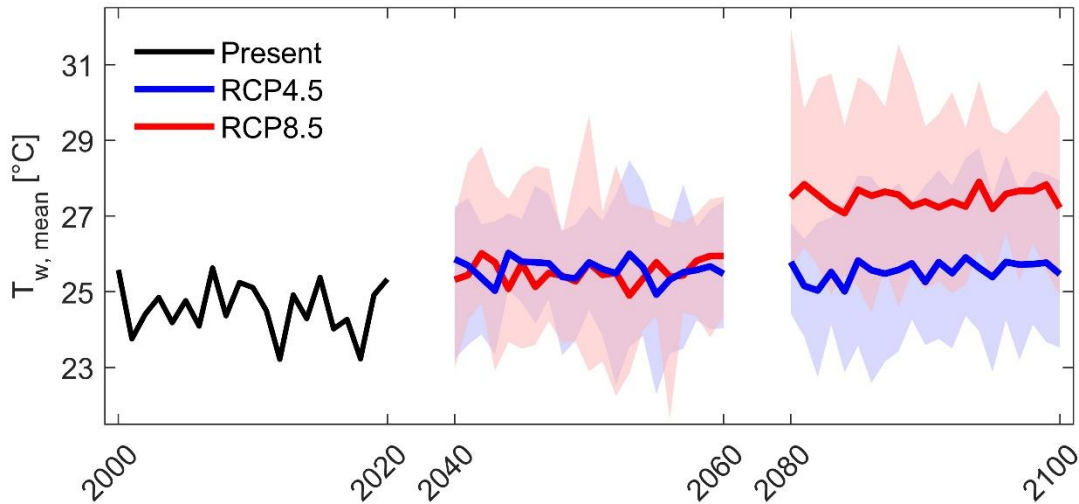


Figure 4: Summer mean air temperature (T_a , upper panel) and total summer precipitation (Pr , lower panel) 1981–2100. The thick black line indicates the observed values, while the thick red and blue lines represent the ensemble means of the climate model simulation results. Thin lines denote individual climate model simulations. All data derived from FORESEE.

265 3.3 Long-term changes in water temperature

Changes in the water temperature were analyzed as a function of time, water depth, and climate scenarios. Since weather was generated with period-specific parameters during forecast to allow the analysis of extreme events (which resulted in statistically homogeneous data with the periods), long-term trends had to be investigated through the mean changes between the stationary periods. Although calculations were performed on a 6-hour basis to better reflect stratification dynamics, the analysis focuses on large-scale changes; therefore, annual summer statistics were used. These considerations apply equally to all subsequent analyses of other variables, too.

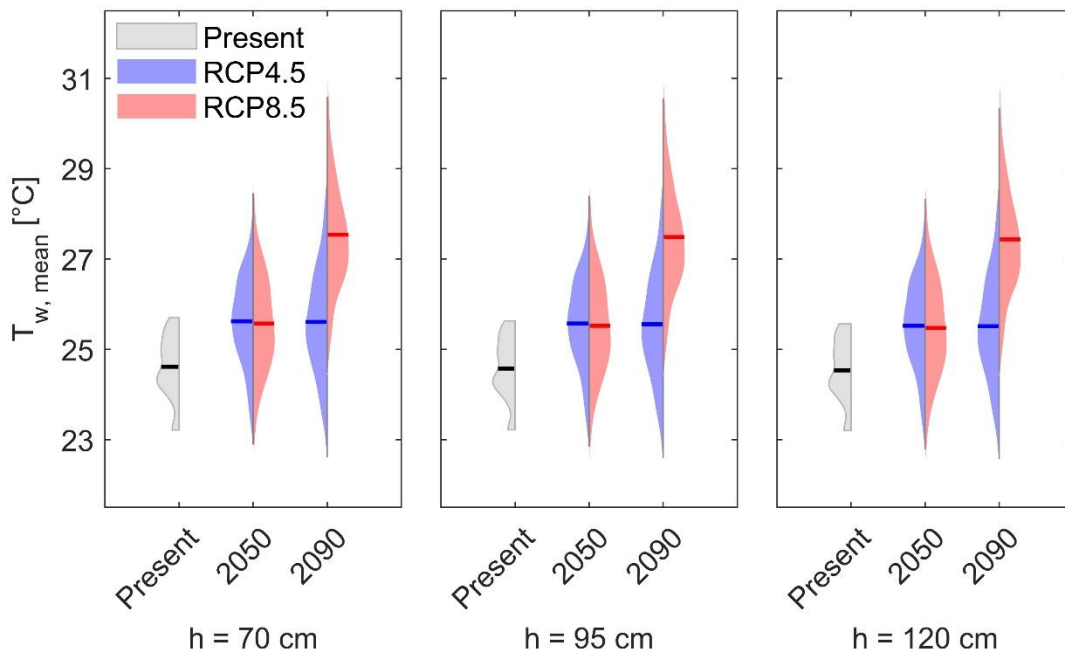
Temporal changes of summer mean water temperatures showed a similar behaviour to air temperature (Fig. 5.); The trajectories of the RCP scenarios are closely aligned until mid-century, but later a substantial divergence developed. There is a comparable magnitude of warming: an increase of approximately 1 °C by the period of 2040-2060 compared to the present conditions, followed by a projected change of 1–2.9 °C by the end of the century, depending on the scenario.



280

Figure 5: Projected changes of the summer mean water temperature (T_w) at 95 cm water level for 2040–2060 and 2080–2100 under RCP4.5 and RCP8.5 climate scenarios. The black bold line represents summer means from the generated present, while blue and red bold lines denote ensemble summer means of 14 climate model results by climate scenario. Shaded areas indicate the range between the minimum and maximum values across the climate model simulations.

Examining the distribution of the annual mean values reveals an increase in the extremes (Fig. 6.), suggesting that higher water temperature is becoming both more frequent and intense, while standard deviations show a temporal increase in variability. The increase in water temperature also affects stratification, leading to stronger and longer stratified periods through the summer (Fig. 8. and 9.). Water depth had a minimal impact on water temperature (Fig. 6.), both in magnitude and distribution.



285

Figure 6: Distribution of the summer mean water temperature ($T_{w,mean}$) for the 2040–2060 and 2080–2100 under RCP4.5 and RCP8.5 by stage (h). Bold lines indicate the mean.

3.4 Changes in stratification

The temporal development of stratification follows a similar increasing trend as air and water temperature regarding RCP scenarios (Fig. 7.). To quantify its changes, we applied medians instead of the means, as the median provides a more robust representation of stratification dynamics, given that mixing periods can significantly distort mean values. In the RCP4.5 scenario, main changes take place until mid-century, followed by a slight decrease. This implies that the lake's stratification tendency is expected to reach its zenith during the first half of the century, with an increase of 0.06-0.09 $J m^{-3}$ compared to the reference period, and remain relatively stable afterwards. In contrast, the RCP8.5 scenario projects a continuous increase of stratification through the end of the century, with a growth of 0.04-0.07 $J m^{-3}$ to 2040-2060, and further 0.1-0.13 $J m^{-3}$ to 2080-2100. Based on the projected air temperature trend, the inflation of stratification tendency is expected to last approximately until the 2090s, after which a decrease may follow. However, the extent of this decrease is uncertain, as the analysis is limited to the period ending in 2100.

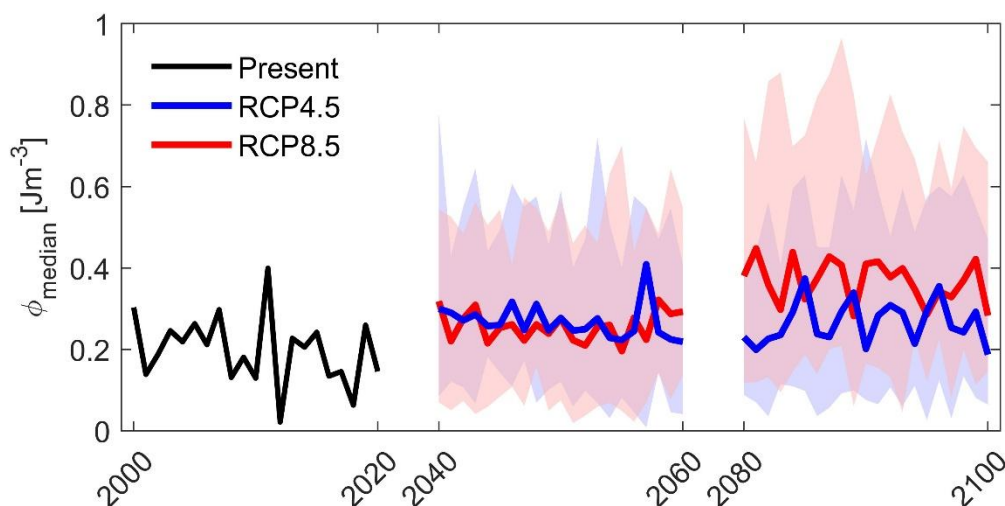


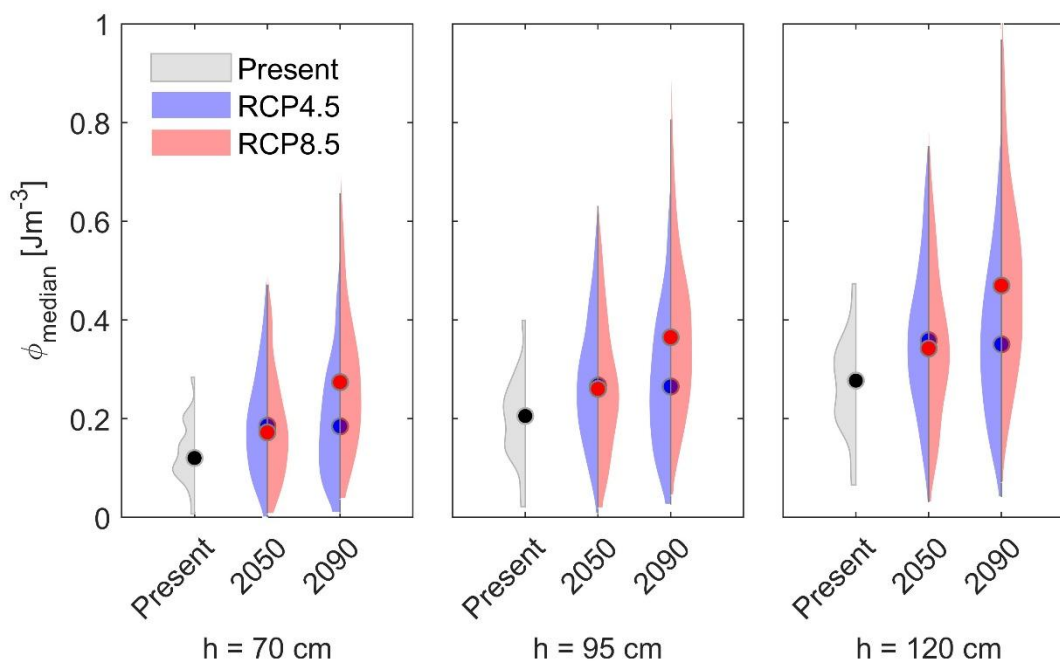
Figure 7: Projected changes of the summer medians of potential energy indices in 2040–2060 and 2080–2100 for 95 cm water level under the RCP4.5 and RCP8.5 climate scenarios. The black bold line represents the summer medians of the generated present, while the blue and red bold lines denote the ensemble means of the summer medians derived from the 14 climate model results, respectively, for the climate scenario. Shaded areas indicate the range between the minimum and maximum.

Although depth did not influence temperature significantly, it still played a crucial role in the development of stratification, with increasing depth strengthening stratification intensity (Fig. 8.). Furthermore, greater depth amplifies the effects of climate change, leading to even stronger stratified periods (Table 2). Therefore, the changes in stratification can be analyzed from two different perspectives: over time and with depth. When temporal variations are assessed as a function of water depth, a decreasing trend is evident in the relative changes in stratification, indicating that with increasing depth, the rate at which stratification intensifies under climate change diminishes. Conversely, when stratification is analyzed over depth as a function



310 of time, a similar decreasing trend is observed, suggesting that the influence of water depth on stratification becomes less pronounced as time progresses.

Relative changes were calculated as a ratio of the mean medians of ϕ between the extreme cases, specifically comparing the present and far future conditions, and the water levels of 70 and 120 cm. Under RCP4.5, ϕ decreases from 2.30 to 1.90 times its present value in the depth-dependent analysis, and from 1.53 to 1.27 times in the time-dependent approach. Under the
 315 RCP8.5, ϕ declines from 2.30 to 1.72 and from 2.28 to 1.70 times its current value in the depth and time-dependent instances, respectively. This indicates that in a predominantly shallow environment, water depth has a crucial influence on stratification, which is comparable to the long-term effects of climate change. A 50 cm increase in water depth is equivalent to, or potentially greater than, the projected impact of climate change by the end of the century, contingent upon the specific RCP scenario. When considering the combined effect of increased water depth and long-term trends, the changes in stratification become
 320 more pronounced. In the most extreme case, where depth changes from 70 to 120 cm by the end of the century, the relative changes in ϕ reach 2.92 and 3.91 times their initial values under the climate scenario, representing a notable increase compared to the previous, less extreme cases.



325 **Figure 8: Violin plots of the summer medians of potential energy anomaly indices (ϕ) for the periods 2040–2060 and 2080–2100 under the RCP4.5 and RCP8.5 climate scenarios for various water levels (h). The dots indicate the medians.**



330

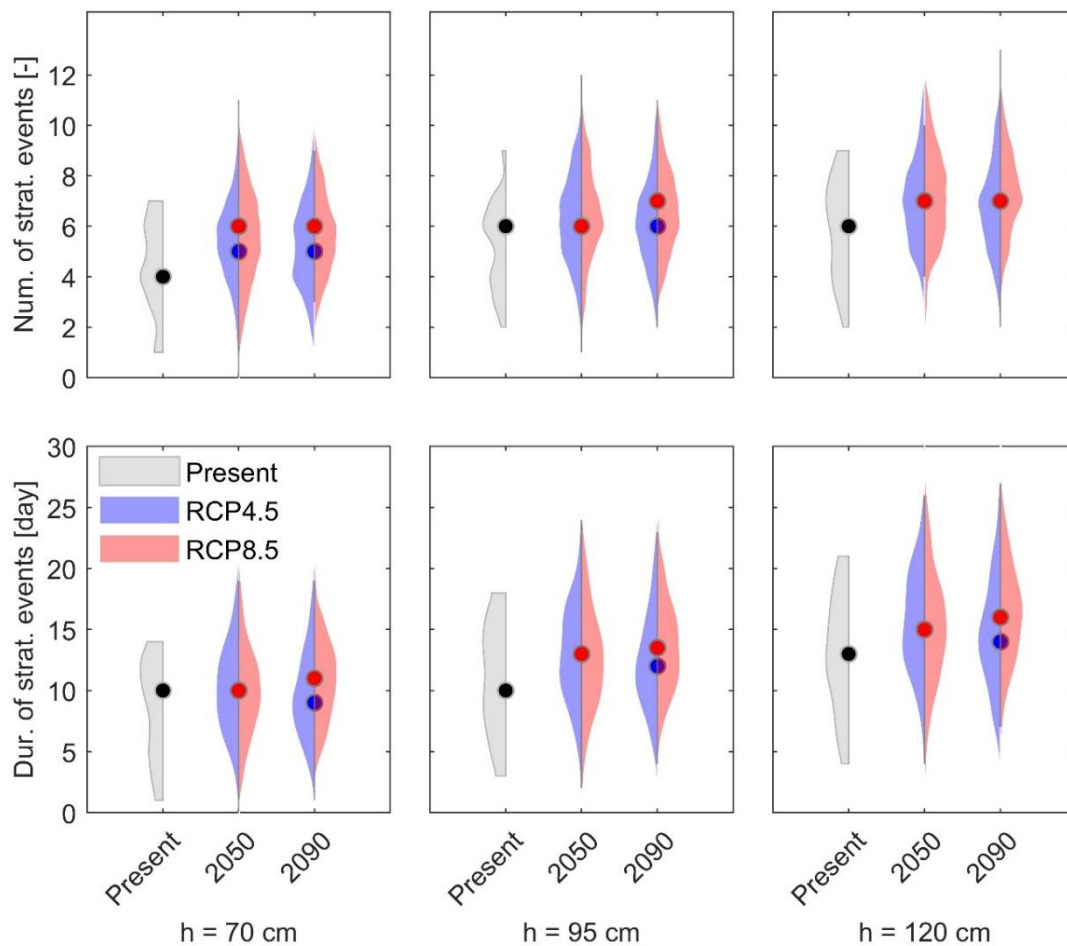
Table 2: Ensemble means \pm standard deviations of the summer medians of potential energy anomaly indices for the periods 2040–2060 and 2080–2100 under the RCP4.5 and RCP8.5 climate scenarios by water level (h). The relative changes of ϕ are shown in bold, all compared to the present conditions. When relative changes are indicated in both cells, they represent the cumulative effect of increased water depth (from 70 to 120 cm) and climate change (from the present to 2080–2100).

	ϕ [J m^{-3}]	h = 70 cm	h = 95 cm	h = 120 cm	rel. change [-]
RCP4.5	Present	0.12 \pm 0.06	0.21 \pm 0.09	0.28 \pm 0.10	2.30 \pm 1.42
	2040-2060	0.19 \pm 0.11	0.27 \pm 0.13	0.36 \pm 0.15	1.93 \pm 1.40
	2080-2100	0.18 \pm 0.12	0.27 \pm 0.14	0.35 \pm 0.16	1.90 \pm 1.51
	rel. change [-]	1.53 \pm 1.26	1.29 \pm 0.89	1.27 \pm 0.74	2.92 \pm 1.97
RCP8.5	2040-2060	0.17 \pm 0.11	0.26 \pm 0.14	0.34 \pm 0.16	1.99 \pm 1.57
	2080-2100	0.27 \pm 0.15	0.36 \pm 0.17	0.47 \pm 0.20	1.72 \pm 1.19
	rel. change [-]	2.28 \pm 1.69	1.78 \pm 1.14	1.70 \pm 0.95	3.91 \pm 2.26

335

340

The number of stratified events and their cumulative duration both showed a slight increase (Fig. 9.). An event was classified as a stable stratification if it persisted for at least 24 hours and exhibited a strength of 0.5 J m^{-3} or higher. In Lake Balaton, this threshold corresponds to a stable stratified state, with a $0.5 \text{ }^\circ\text{C}$ difference between the water surface and bottom. From a temporal perspective, the number of stratified events is projected to increase by 0 to 2 events per summer by the end of the century, while from a depth-related aspect, an increase of 1 to 2 events per summer is anticipated in both RCP scenarios (Table 3). The duration of these events is likewise expected to increase by approximately 0-3 days per summer throughout the examined periods, while along depth, a 3-5 days increase is projected in response to the climate scenarios. For the number of stratified events, the effects of water depth and climate change are nearly equivalent; however, in terms of duration, the former has a slightly greater impact, leading to longer stratified periods. The comparison of the RCP scenarios indicates no substantial differences overall, despite the significant disparities observed in the projected stratification strengths. This suggests that although stratification intensity is projected to increase, the magnitude of this increase remains insufficient to substantially counteract wind-driven mixing processes and therefore does not lead to notably more frequent or prolonged stratified events.



345 **Figure 9:** Distribution of the number of summer stratified events (upper) and their cumulative duration (lower) for the periods 2040–2060 and 2080–2100 under the RCP4.5 and RCP8.5 climate scenarios for various water levels (h). The dots indicate the medians of the datasets.

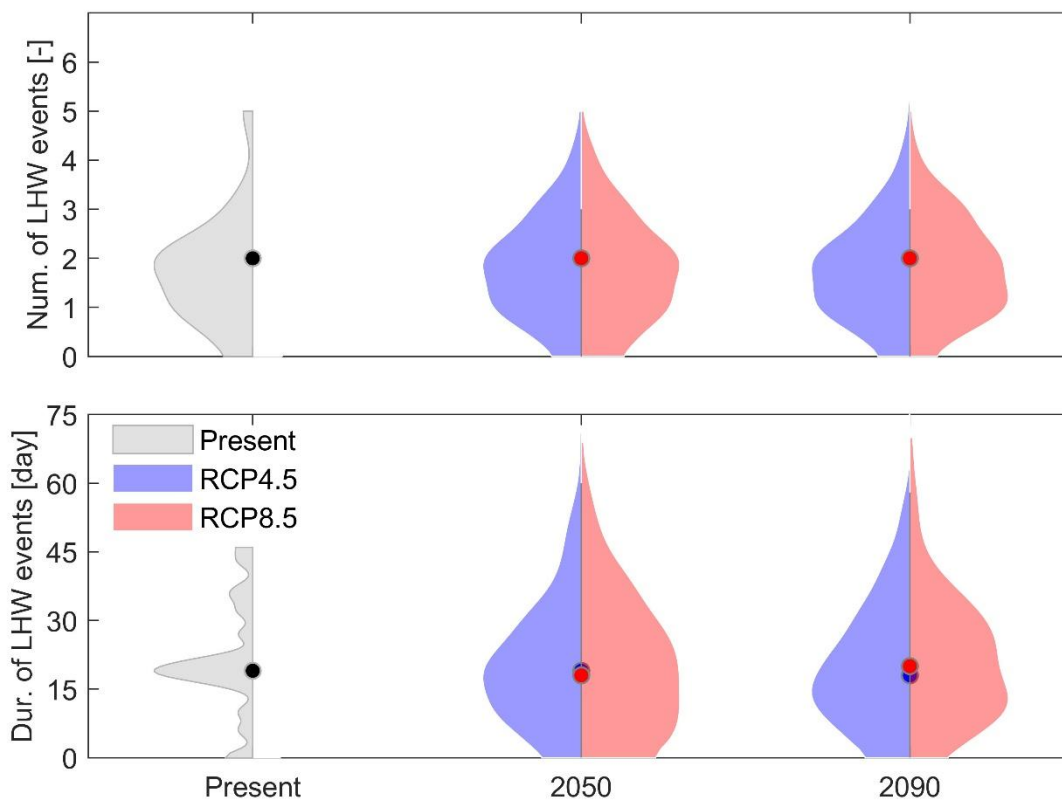


350 **Table 3: Ensemble means and distributions of the summer medians of the number of summer stratified events and their cumulative durations for the periods 2040–2060 and 2080–2100 under the RCP4.5 and RCP8.5 climate scenarios by water level (h).**

		h = 70 cm	h = 95 cm	h = 120 cm	
Num. of strat. events [-]	Present	4 ± 2	6 ± 2	6 ± 2	
	RCP4.5	2040-2060	5 ± 2	6 ± 2	7 ± 2
		2080-2100	6 ± 2	6 ± 2	7 ± 2
	RCP8.5	2040-2060	5 ± 2	6 ± 2	7 ± 2
		2080-2100	6 ± 2	7 ± 2	7 ± 2
	Dur. of strat. events [day]	Present	10 ± 4	10 ± 5	13 ± 5
RCP4.5		2040-2060	10 ± 4	13 ± 4	15 ± 5
		2080-2100	10 ± 4	13 ± 5	15 ± 5
RCP8.5		2040-2060	9 ± 4	12 ± 5	14 ± 5
		2080-2100	11 ± 4	13 ± 5	16 ± 5

3.5 Lake heatwaves

As lake heatwaves were calculated from vertically averaged water temperatures, water depth has negligible effect on them; Therefore, the relative changes in their frequency and duration were solely evaluated over time. There is no significant difference in either the number of lake heatwave events or in their cumulative durations across the different time periods and RCP scenarios (Fig. 10.). On average, approximately two heatwave events occur each summer across all cases, with a median duration ranging from 18 to 20 days. Similarly, other statistical metrics, including standard deviation and the 10th and 90th percentiles, exhibit no substantial differences between the cases (Table 4). The only notable deviation is in the RCP8.5 scenario for 2040–2060, where the 10th percentile of summer lake heatwave duration is 0 days compared to 6 days in other cases. However, this discrepancy is likely attributable to the stochastic nature of the data, as all other metrics remain consistent and do not indicate systematic changes. In contrast, the maximum durations show a notable deviation from present conditions. Nevertheless, the consistency of the mean, standard deviation, and the 10th and 90th percentiles indicates that the overall distribution of lake heatwave characteristics remains largely stable over time. This suggests that while rare extremes may occur in the future, the typical summer behavior of heatwaves is not substantially affected.



365 **Figure 10: Distribution of the number of lake heatwave (LHW) events (upper) and their cumulative durations (lower) for the periods 2040–2060 and 2080–2100 under the RCP4.5 and RCP8.5 climate scenarios at the water level of 95 cm. The dots indicate the medians of the datasets.**

Table 4: Ensemble means of the medians and standard deviations of summer lake heatwave event duration, along with the 10th and 90th percentiles and the maximum values under the RCP4.5 and RCP8.5 climate scenarios at a water level of 95 cm.

		Median	10 th percentile	90 th percentile	Maximum	
Dur. of LWH events [days]	Present	19 ± 12	6	37	46	
	RCP4.5	2040-2060	19 ± 13	5	40	71
		2080-2100	18 ± 14	5	39	81
	RCP8.5	2040-2060	18 ± 14	0	40	69
		2080-2100	20 ± 13	6	38	70

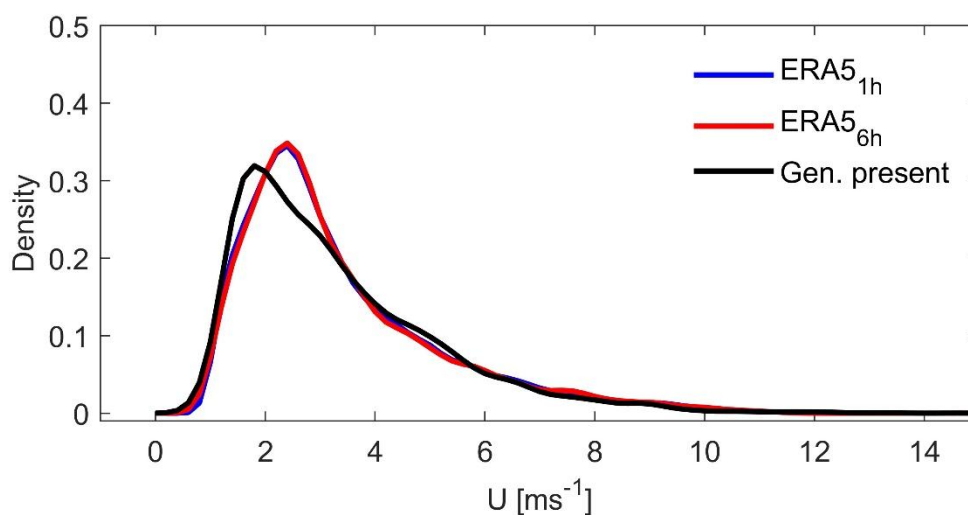
370



4 Discussion

4.1 Modeling uncertainty

The primary source of uncertainty in modeling arises from the downscaling and generation of wind speed data, which is the
375 main driving force of lake mixing. Wind forecasting poses substantial challenges within atmospheric modeling frameworks,
primarily due to the intermittent, highly turbulent, and nonlinear nature of wind variability (Shu et al., 2021; Sfetsos, 2000).
Through downscaling, the generated wind speed data exhibit a distribution similar to that of the ERA5 hourly and six-hourly
datasets; however, even after bias correction, some discrepancies remain. Comparison of the probability density functions (Fig.
11.) indicates that the hourly and six-hourly ERA5 distributions are nearly identical, reflecting the subsampling of the latter
380 from the former. In contrast, the generated wind speed data shows a slightly lower peak and a shift toward lower wind speeds.
In terms of range, the generated dataset spans a broader interval, exhibiting both higher and lower extreme wind speed values
compared to the other datasets. The slightly lower peak and the shift toward weaker wind speeds in the generated dataset may
lead to an underestimation of wind-driven mixing, potentially resulting in more persistent and stronger thermal stratification
periods. Conversely, the broader range and enhanced extremes may intensify mixing, promoting weaker and shorter
385 stratifications; however, such events are likely to have a limited influence due to their low probability of occurrence.
Nevertheless, the uncertainties associated with these effects are to some extent counterbalanced by the application of bias
correction to the modeled water temperatures and potential energy anomaly indices. Thus, while uncertainties are introduced
during the wind speed generation process, their effects are mitigated through the post-processing and are unlikely to persist in
the results.



390

Figure 11: Comparison of the probability density functions (kernel density estimates) of wind speed derived from the hourly ERA5, six-hourly ERA5, and FORESEE downscaled (generated) data for the baseline period of 2000-2020.



A slight decrease can be observed in the relative changes in projected wind speeds by the mid-century, which becomes somewhat more pronounced over time, depending on the climate scenario. Under RCP4.5, the annual summer mean wind speed decreases from 3.30 to 3.26 m s⁻¹ during 2040-2060 and remains largely unchanged thereafter, whereas under RCP8.5 a gradual decline is projected, reaching 3.27 and 3.19 m s⁻¹ in the respective future periods. Probability density functions further indicate a systematic shift toward lower summer means, with only minor changes in distribution shape (not shown here), suggesting the persistence of prevailing wind regimes at slightly reduced intensity. Although the decreases in speeds are modest – 1.2-3.3% by the end of the century –, they are consistent with observed historical declines (Spinoni et al., 2015) and regional projections for the Carpathian Basin (Tobin et al., 2015). However, the magnitude of these changes remains uncertain and may still exert a significant influence on stratification conditions.

4.2 Ecological implications

The solubility of dissolved oxygen in water decreases with increasing water temperatures, thus warming reduces the availability of oxygen for aquatic ecosystems. Therefore, the projected rise in Lake Balaton's water temperature over the 21st century is expected to result in lower dissolved oxygen concentrations within the lake, especially when the lower water layers are isolated from the atmosphere by thermal stratification. Consequently, the risk of oxygen depletion occurring is likely to increase, potentially intensifying internal nutrient loading (Istvánovics et al., 2022) and contributing to more frequent algal blooms and fish mortality. Furthermore, changes in water temperature also affect the lake's ecosystem by altering the composition of species, with warm-tolerant species likely to gain more ground. Elevated temperature additionally influences growth-related processes, such as the timing of growth onset and the final attained body sizes (Mooij et al., 2008). Overall, the increase in water temperature has several consequences that necessitate a comprehensive understanding of climate change impacts for sustainable and long-term water management.

Honti et al. (2025) investigated changes in Lake Balaton's natural water balance through the end of the century and found that it is projected to turn negative gradually. They evaluated the changes using the RCP4.5 and RCP8.5 climate scenarios for 24 climate models, using their ensembles to assess the projected future impacts. In both scenarios, the lake's water level will drop significantly, even if only temporarily, indicating the importance of an external water transfer, which is currently unresolved. Based on their findings, it can be assumed that after 2040, the frequency of lower water levels will increase and become a prevailing hydrological state throughout the remainder of the century, with consequential impacts on the lake's thermal stratification. The declining water levels are expected to weaken stratification, although the influence of climate change will remain significant (Tables 2 and 3). Consequently, without water transfer, the lake's stratification is likely to remain relatively unchanged or decline compared to its current intensive stratification tendency, with corresponding changes in the frequency of stratified events.

In addition to these projected changes, most studies indicate that lake heatwaves will become more frequent by the end of the century, a trend consistent with rising air and water temperatures. Such projections, however, often rely on present-day or historical periods as reference baselines. Accordingly, the changes calculated in this way quantify deviations relative to those



conditions, serving as indicators for anticipating future climatic trends and their expected impacts on contemporary ecosystems. Nevertheless, this baseline-dependent approach cannot fully capture how lake heatwave anomalies and their behavior may evolve, as continued warming inherently implies an overall upward trend. To investigate expected changes in heatwave anomalies, redefinition of the climatological baseline relative to the evolving thermal regime may be a viable
430 approach. By accounting for shifts in the climatological mean, changes in heatwave anomalies may be characterized more precisely, thereby enabling investigation of how heatwave frequencies may evolve under future climate conditions and facilitating assessment of their broader impacts. In the case of Lake Balaton, the frequency and duration of lake heatwave events are expected to remain relatively stable, with no significant changes. Nevertheless, rare extremes may occur in the future, imposing substantially greater stress on the lake's ecosystem than is currently observed.

435 **5 Conclusions**

The long-term impacts of climate change on the thermal stratification of shallow polymictic lakes are largely unexplored, as the predominantly daily or coarser resolution of climate model results limits the direct representation of intra-daily stratification processes. This study aimed to address this gap by introducing a modeling framework that enables the downscaling of meteorological data and the simulation of lake thermal properties at sub-daily temporal resolution, thereby supporting the
440 quantification of the impact of future climate projections.

Model forecasts show that the effects of climate change on lake stratification are strongly modulated by water depth, with its relative impact diminishing as depth increases. Conversely, when examined over time, the influence of water depth weakens, such that the temporal intensification of climate change effects on the lake's stratification becomes progressively less pronounced. When their synergistic interaction is considered, stratification changes exceed those arising from each factor
445 acting independently, indicating an overall amplification.

The number and duration of stratified events indicates that wind forcing will remain a dominant factor in regulating stratification dynamics, even under the projected future warming. Although both metrics show a slight increase toward the end of the century, the projected strengthening of stratification is insufficient to substantially counteract wind-driven mixing and therefore does not translate into markedly more frequent or prolonged stratified events under either climate scenario.

450 Lake heatwave characteristics are projected to remain largely stable over time, indicating no substantial changes in either their distribution or mean statistics. Although extreme events may occur in the future, the typical summer behavior of lake heatwaves is not expected to change.

Lastly, the presented modeling framework was shown to be suitable for simulating stratification dynamics in shallow, polymictic systems, where sub-daily temporal resolution is required to adequately capture the system dynamics. The results
455 demonstrate that future assessments should consider the interplay between climate change and water depth in controlling stratification dynamics when evaluating long-term management and adaptation strategies for shallow lake systems.



Code and data availability

The FORESEE dataset used for this work can be accessed at <https://meteordata.elte.hu/FORESEE/index.html>, while the one-dimensional GOTM model at <https://gotm.net/portfolio/>. The ERA5 dataset can be reached at
460 <https://cds.climate.copernicus.eu/datasets/reanalysis-era5-land?tab=overview>, while the applied weather generator is available from the authors upon request.

Author contributions

ST: Writing (original draft preparation), Conceptualization, Data curation, Formal analysis, Methodology, Investigation, Software, Validation, Visualization, Funding acquisition
465 MH: Writing (review and editing), Methodology, Software
PT: Writing (review and editing), Supervision, Conceptualization, Formal analysis, Funding acquisition

Competing interests

The authors declare that they have no conflict of interest.

Financial support

470 The research was carried out within the framework of the Szechenyi Plan Plus program with the support of the RRF 2.3.1 21
2022 00008 project. It was also funded by the Ministry of Culture and Innovation and the National Research, Development and Innovation Office (Grant Nr: TKP2021-NVA-02). Sebestyén Török was supported by the Doctoral Excellence Fellowship Programme (DCEP) funded by the National Research Development and Innovation Fund of the Ministry of Culture and Innovation and the Budapest University of Technology and Economics, under a grant agreement with the National Research,
475 Development and Innovation Office. Péter Torma was supported by the Hungarian Academy of Sciences (Award: Janos Bolyai fellowship 00906/23).

References

Adrian, R., O'Reilly, C.M., Zagarese, H., Baines, S.B., Hessen, D.O., Keller, W., Livingstone, D. M., Sommaruga, R., Straile, D., Van Donk, E., Weyhenmeyer, G. A., Winder, M.: Lakes as sentinels of climate change, *Limnology and*
480 *Oceanography*, 54 (6), 2283-2297, https://doi.org/10.4319/lo.2009.54.6_part_2.2283, 2009.
Burchard, H., Bolding, K., Ruiz-Villarreal, M.: GOTM, a general ocean turbulence model. Theory, implementation and test cases, Report EUR 18745, European Commission, Brussels, Belgium, 1999.



- Cowpertwait, P. S. P.: Further developments of the Neyman-Scott clustered point process for modeling rainfall, *Water Resour. Res.*, 27, 1431–1438, <https://doi.org/10.1029/91WR00479>, 1991.
- 485 Clark, N. E., Eber, L., Laurs, R. M., Renner, J. A., Saur, J. F. T.: Heat exchange between ocean and atmosphere in the Eastern North Pacific for 1961-1971, Tech. Rep. NMFS SSRF682, NOAA, U.S. Dept. of Commerce, Washington, D.C., 1974.
- Favre, A-C., Musy, A., Morgenthaler, S.: Unbiased parameter estimation of the Neyman-Scott model for rainfall simulation with related confidence interval, *Journal of Hydrology*, 286 (1–4), 168-178, <https://doi.org/10.1016/j.jhydrol.2003.09.025>, 2004.
- 490 Fukushima, T., Matsushita, B., Sugita, M.: Quantitative assessment of decadal water temperature changes in Lake Kasumigaura, a shallow turbid lake, using a one-dimensional model, *Science of The Total Environment*, 845, 157247, <https://doi.org/10.1016/j.scitotenv.2022.157247>, 2022.
- Hetherington, A. L., Schneider, R. L., Rudstam, L. G., Gal, G., DeGaetano, A. T., Walter, M. T.: Modeling climate change impacts on the thermal dynamics of polymictic Oneida Lake, New York, United States, *Ecological Modelling*, 300, 1-11, <https://doi.org/10.1016/j.ecolmodel.2014.12.018>, 2015.
- 495 Hobday, A. J., Alexander, L. V., Perkins, S. E., Smale, D. A., Straub, S. C., Oliver, E. C. J., Benthuisen, J. A., Burrows, M. T., Donat, M. G., Feng, M., Holbrook, N. J., Moore, P. J., Scannell, H. A., Gupta, A. S., Wernberg, T.: A hierarchical approach to defining marine heatwaves, *Progress in Oceanography*, 141, 227-238, <https://doi.org/10.1016/j.pocean.2015.12.014>, 2016.
- Honti, M., Istvánovics, V., Berecz, D., Fülöp, B., Herodek, S.: Water transfer to Lake Balaton: To do, but when and what?, *Hungarian Journal of Hydrology*, 105 (1), 6-22, <https://doi.org/10.59258/hk.18346>, 2025. (in Hungarian)
- 500 IPCC: Climate Change 2014: Synthesis Report. Contribution of Working Groups I, II and III to the Fifth Assessment Report of the Intergovernmental Panel on Climate Change, IPCC, Geneva, Switzerland, 2014.
- Istvánovics, V., Honti, M.: Coupled simulation of high-frequency dynamics of dissolved oxygen and chlorophyll widens the scope of lake metabolism studies, *Limnology and Oceanography*, 63 (1), 72-90, <https://doi.org/10.1002/lno.10615>, 2018.
- 505 Istvánovics, V., Honti, M., Torma, P., Kousal, J.: Record-setting algal bloom in polymictic Lake Balaton (Hungary): A synergistic impact of climate change and (mis)management, *Freshwater Biology*, 67(6), 1091-1106, <https://doi.org/10.1111/fwb.13903>, 2022.
- Jane, S. F., Hansen, G. J. A., Kraemer, B. M., et al.: Widespread deoxygenation of temperate lakes. *Nature*, 594 (7861), 66–70, <https://doi.org/10.1038/s41586-021-03550-y>, 2021.
- 510 Kern, A., Dobor, L., Hollós, R., Marjanovic, H., Torma, Cs.Zs., Kis, A., Fodor, N., Barcza, Z.: Seamlessly combined historical and projected daily meteorological datasets for impact studies in Central Europe: the FORESEE v4.0 and the FORESEE-HUN v1.0, *Climate Services*, 33, 100443, <https://doi.org/10.1016/j.cliser.2023.100443>, 2024.
- Kilsby, C.G., Jones, P.D., Burton, A., Ford, A.C., Fowler, H.J., Harpham, C., James, P., Smith, A., Wilby, R.L.: A daily weather generator for use in climate change studies, *Environmental Modelling and Software*, 22 (12), 1705–1719, <https://doi.org/10.1016/j.envsoft.2007.02.005>, 2007.
- 515



- Kimura, N., Wu, C. H., Hoopes, J. A., Tai, A.: Diurnal Dynamics in a Small Shallow Lake under Spatially Nonuniform Wind and Weak Stratification. *Journal of Hydraulic Engineering*, *142*(11), 04016047, [https://doi.org/10.1061/\(ASCE\)HY.1943-7900.0001190](https://doi.org/10.1061/(ASCE)HY.1943-7900.0001190), 2016.
- 520 Kondo, J.: Air-sea bulk transfer coefficients in diabatic conditions, *Boundary-Layer Meteorology*, *9*, 91-112, <https://doi.org/10.1007/BF00232256>, 1975.
- La Fuente, S., Jennings, E., Lenters, J. D., Verburg, P., Kirillin, G., Shatwell, T., Couture, R.-M., Côté, M., Vinnå, C. L. R., Woolway, R. I.: Increasing warm-season evaporation rates across European lakes under climate change, *Climatic Change*, *177*, 173, <https://doi.org/10.1007/s10584-024-03830-2>, 2024.
- Martinsen, K. T., Andersen, M. R., Sand-Jensen, K., 2019. Water temperature dynamics and the prevalence of daytime stratification in small temperate shallow lakes. *Hydrobiologia*, *826*, 247–262. <https://doi.org/10.1007/s10750-018-3737-2>
- 525 Mooij, W. M., De Senerpont Domis, L. N., Hülsmann, S.: The impact of climate warming on water temperature, timing of hatching and young-of-the-year growth of fish in shallow lakes in the Netherlands, *Journal of Sea Research*, *60* (1–2), 32-43, <https://doi.org/10.1016/j.seares.2008.03.002>, 2008.
- Rodriguez-Iturbe, I., Cox, D.R., Isham, V.: Some models for rainfall based on stochastic point processes. *Proceedings of the Royal Society of London Series A*, *410* (1839), 269-288, <https://doi.org/10.1098/rspa.1987.0039>, 1987.
- 530 Sahoo, G. B., Forrest, A. L., Schladow, S. G., Reuter, J. E., Coats, R., & Dettinger, M.: Climate change impacts on lake thermal dynamics and ecosystem vulnerabilities, *Limnology and Oceanography*, *61*(2), 496–507, <https://doi.org/10.1002/lno.10228>, 2016.
- Salmaso N.: Effects of climatic fluctuations and vertical mixing on the interannual trophic variability of Lake Garda, Italy, *Limnology and Oceanography*, *50* (2), 553–565, <https://doi.org/10.4319/lo.2005.50.2.0553>, 2005.
- 535 Schwalm, C.R., Glendon, S., Duffy, P.B.: RCP8.5 tracks cumulative CO2 emissions, *Proceedings of the National Academy of Sciences U.S.A.*, *117* (33), 19656-19657, <https://doi.org/10.1073/pnas.2007117117>, 2020.
- Schwefel, R., Nkwilale, L.G.T., Jordan, S., Rinke, K., Hupfer, M.: Temperatures and hypolimnetic oxygen in German lakes: Observations, future trends and adaptation potential, *Ambio*, *54*, 428–447, <https://doi.org/10.1007/s13280-024-02046-z>, 2025.
- 540 Sfetsos, A.: A comparison of various forecasting techniques applied to mean hourly wind speed time series. *Renewable Energy*, *21* (1), 23-35, [https://doi.org/10.1016/S0960-1481\(99\)00125-1](https://doi.org/10.1016/S0960-1481(99)00125-1), 2000.
- Shatwell, T., Thiery, W., and Kirillin, G.: Future projections of temperature and mixing regime of European temperate lakes, *Hydrol. Earth Syst. Sci.*, *23*, 1533–1551, <https://doi.org/10.5194/hess-23-1533-2019>, 2019.
- Shi, J., Wang, L., Yang, Y., Huang, T.: A case study of thermal and chemical stratification in a drinking water reservoir, *Science of The Total Environment*, *848*, 157787, <https://doi.org/10.1016/j.scitotenv.2022.157787>, 2022.
- 545 Shu, Z. R., Chan, P. W., Li, Q. S., He, Y. C., Yan, B. W.: Investigation of chaotic features of surface wind speeds using recurrence analysis, *Journal of Wind Engineering and Industrial Aerodynamics*, *210*, 104550, <https://doi.org/10.1016/j.jweia.2021.104550>, 2021.



- Smith, E. T., Diaz D. B., Mardian, J.: A Climate-Informed Approach to Create Hourly Future Weather Timeseries for Power
550 System Planning, *IEEE Access*, 13, 82796-82806, [10.1109/ACCESS.2025.3567864](https://doi.org/10.1109/ACCESS.2025.3567864), 2025.
- Spinoni, J., Szalai, S., Szentimrey, T., Lakatos, M., Bihari, Z., Nagy, A., et al.: Climate of the Carpathian region in the period
1961–2010: climatologies and trends of 10 variables. *Int. J. Climatol*, 35, 1322–1341, <https://doi.org/10.1002/joc.4059>, 2015.
- Tobin, I., Vautard, R., Balog, I. *et al.*: Assessing climate change impacts on European wind energy from ENSEMBLES high-
resolution climate projections, *Climatic Change*, 128, 99–112, <https://doi.org/10.1007/s10584-014-1291-0>, 2015.
- 555 Torma, P., Krámer, T.: Modeling the Effect of Waves on the Diurnal Temperature Stratification of a Shallow Lake, *Periodica
Polytechnica Civil Engineering*, 61(2), 165–175, <https://doi.org/10.3311/PPci.8883>, 2017.
- Török, S. D., Torma, P.: Long-term changes in summer stratification of a shallow polymictic lake by climate change and
anthropogenic water level regulation, *Science of The Total Environment*, 1009, 181025,
<https://doi.org/10.1016/j.scitotenv.2025.181025>, 2025.
- 560 Török, S. D., Torma, P.: Prediction of long-term changes of weak diurnal stratification in shallow lakes using artificial neural
networks, *Journal of Water and Climate Change*, 15 (8), 3724-3737, <https://doi.org/10.2166/wcc.2024.032>, 2024.
- Török, S., Torma, P., Weidinger, T.: Characterization and impact of heat exchange at the sediment-water interface in Lake
Balaton. *Hungarian Journal of Hydrology*, 103 (3), 33-43, 2023. (in Hungarian)
- Woolway, R. I., Kraemer, B. M., Lenters, J. D., Merchant, C. J., O'Reilly, C. M., Sharma, S.: Global lake responses to climate
565 change, *Nature Reviews Earth & Environment*, 1(8), 388-403, <https://doi.org/10.1038/s43017-020-0067-5>, 2020.
- Woolway, R.I., Jennings, E., Shatwell, T., Golub, M., Pierson, D. C., Maberly S. C.: Lake heatwaves under climate
change. *Nature*, 589, 402–407, <https://doi.org/10.1038/s41586-020-03119-1>, 2021a.
- Woolway, R.I., Sharma, S., Weyhenmeyer, G.A. et al.: Phenological shifts in lake stratification under climate change. *Nat
Commun*, 12, 2318, <https://doi.org/10.1038/s41467-021-22657-4>, 2021b.